Author(s): Kuosmanen, Riikka; Puttreddy, Rakesh; Willman, Roosa-Maria; Äijäläinen, Ilkka; Galandáková, Adéla; Ulrichová, Jitka; Salo, Hannu; Rissanen, Kari; Sievänen, Elina

Title: Biocompatible Hydrogelators Based on Bile Acid Ethyl Amides

Year: 2016

Version:

Please cite the original version:

Kuosmanen, R., Puttreddy, R., Willman, R.-M., Äijäläinen, I., Galandáková, A., Ulrichová, J., Salo, H., Rissanen, K., & Sievänen, E. (2016). Biocompatible Hydrogelators Based on Bile Acid Ethyl Amides. Steroids, 108, 7-16. https://doi.org/10.1016/j.steroids.2016.02.014

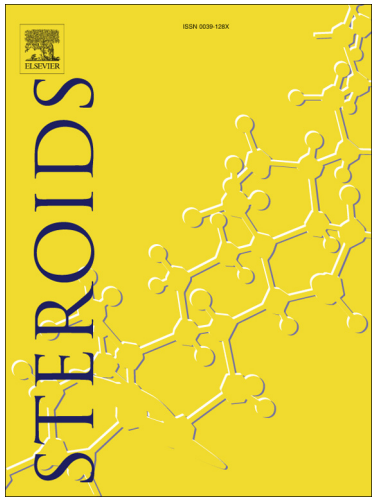

Biocompatible Hydrogelators Based on Bile Acid Ethyl Amides

Riikka Kuosmanen, Rakesh Puttreddy, Roosa-Maria Willman, Ilkka Äijäläinen, Adéla Galandáková, Jitka Ulrichová, Hannu Salo, Kari Rissanen, Elina Sievänen

PII: S0039-128X(16)00045-3
DOI: http://dx.doi.org/10.1016/j.steroids.2016.02.014
Reference: STE 7931

To appear in: *Steroids*

Received Date: 1 December 2015
Revised Date: 15 February 2016
Accepted Date: 18 February 2016

Please cite this article as: Kuosmanen, R., Puttreddy, R., Willman, R-M., Äijäläinen, I., Galandáková, A., Ulrichová, J., Salo, H., Rissanen, K., Sievänen, E., Biocompatible Hydrogelators Based on Bile Acid Ethyl Amides, *Steroids* (2016), doi: http://dx.doi.org/10.1016/j.steroids.2016.02.014

Biocompatible Hydrogelators Based on Bile Acid Ethyl Amides

Riikka Kuosmanen, Rakesh Puttreddy, Roosa-Maria Willman, Ilkka Äijäläinen, Adéla Galandáková, Jitka Ulrichová, Hannu Salo, Kari Rissanen, and Elina Sievänen*

University of Jyvaskyla, Department of Chemistry, P.O.Box 35, FI-40014 University of Jyvaskyla, Finland

Abstract

Four novel bile acid ethyl amides were synthetized using a well-known method. All the four compounds were characterized by IR, SEM, and X-ray crystal analyses. In addition, the cytotoxicity of the compounds was tested. Two of the prepared compounds formed organogels. Lithocholic acid derivative **1** formed hydrogels as 1 % and 2 % (w/v) in four different aqueous solutions. This is very intriguing regarding possible uses in biomedicine.

Keywords: Bile acid, Amide, Self-assembly, Supramolecular hydrogel, Biocompatibility

1. Introduction

Bile acids are a fascinating group of biologically important molecules belonging to the group of steroids.[1,2] Because of their relatively low cost, wide availability, and enantiomeric purity, bile acids are ideal building blocks for gelator molecules. The structure of the bile acids consists of a steroidal backbone and an aliphatic side chain.[3] The facially amphiphatic nature of bile acids arises from their concave hydrophilic face and convex hydrophobic face. Chemically different hydroxyl groups in the concave face and the varying amount of them, as well as the rigid steroidal backbone, are important with regard to bile acids' biological etc. properties. Because bile acids are endogenous compounds[4], they are perfect starting materials for biological and medical applications.[3,5]

Bile acids and their derivatives have various applications especially in biomedicine. There are multiple examples in the field of cancer treatment.[6–11] One particularly interesting potential application involves mixing of sodium deoxycholate solutions to Au-nanoparticle (AuNP) solution to create multiple-branched Au-NPs.[8] AuNPs formed have such a strong NIR absorption that they

can be used to destroy tumor cells. Many examples include bile acid based compounds as drug carriers[12–17], and even gene[18,19] or RNA[20] carriers. Majority of potential applications of bile acids, or their derivatives, as drug carriers utilize bile acid transportation systems present in organisms/humans to achieve site-specific action of the drug carried. In addition, bile acid derivatives have shown potential as drug absorption modifiers.[21,22]

Gels play increasingly important roles in modern life since they appear in myriad of applications ranging from optoelectronics[23,24] and biomedicine[23–25] to environmental clean-up.[26,27] Universally a gel is defined as a viscoelastic solid like material which consists of flexible cross-linked network and solvent. Gelator molecules form the cross-linked 3D network that attracts and captures solvent molecules. Gels are divided into different classes based on the solvent used. In hydrogels the solvent is pure water or water solution. If the solvent is organic, the gel is called an organogel, and dried gels are categorized as xerogels.

In the field of supramolecular gels the research focuses mainly on low molecular weight gelators (LMWG).[28] Typically LMWGs form gel networks that resemble fibres. LMWGs consist of a rich variety of molecules to which bile acids and their derivatives enter into.

The first examples of bile acid salts forming hydrogels were reported in the early 20th century.[29–31] Despite of that there is a limited amount of bile acid salts and derivatives known to function as hydrogelators. Most of the bile acid based hydrogels reported have been discovered by Maitra and his co-workers. Maitra's research group has reported intriguing gel systems, including cholic acid based luminescent europium containing gels and tripodal cholamide supergelator. This is, however, the first time bile acid alkyl amide derivatives are reported to gelate aqueous solutions.

Gels have potential use in biological applications only if they form in biocompatible solvents. Supramolecular hydrogels are considered to be biologically compatible, moreover they are formed in many cases by naturally occurring molecules which are most likely to be nontoxic.[32] Bile acid based hydrogels are considered to be fully biologically compatible when the gelator molecule itself is not toxic. The full biocompatibility of a hydrogel provides perhaps new potential applications regarding biomedicine, such as drug delivery, artificial tissue engineering, etc.

In relation to the previous work done by our research group[33–40], in this work we have focused on how the compounds we have prepared behave in aqueous media. As a continuation of the series of bile acid alkyl or functionalized alkyl amide/ester derivatives capable of acting as gelators we report

four new bile acid ethyl amide based gelator molecules, which have shown potential in forming hydrogels.

2. Experimental

2.1 Materials

Lithocholic acid (≥97 %), deoxycholic acid (≥99 %), cholic acid (≥97 %), and dehydrocholic acid (≥99.0 %) were purchased from Sigma. Ethyl amide hydrochloride was purchased from Fluka. Triethyl amide, ethyl chloroformate, and other reagents used during the synthesis as well as solvents used in chromatography and gelation studies were of analytical grade. Ethyl chloroformate was distilled and 1,4-dioxane was dried over Na prior to use. All other chemicals were used without further purification. The synthetic route to **1**–**4** is presented in Scheme 1. The mixed anhydride method used has been previously reported by our research group.[41]

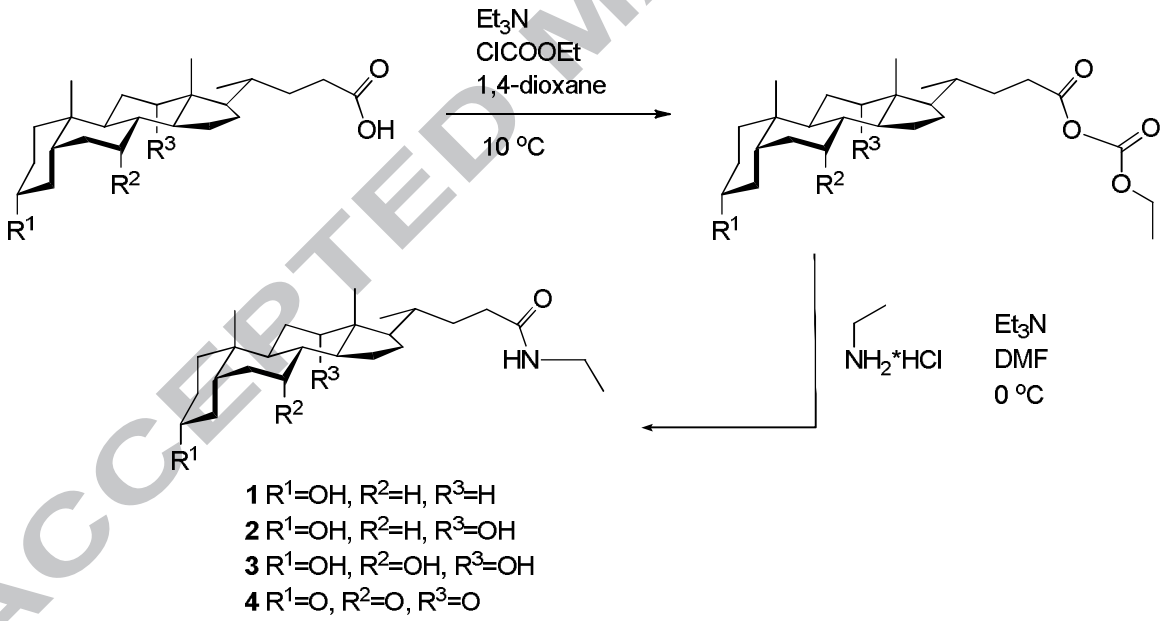

Scheme 1: The synthetic route leading to compounds **1**–**4**.

2.2 General procedure for the synthesis of the bile acid ethyl amide conjugates **1**–**4**

Reactions were performed under N_2 atmosphere. In a round-bottomed three-necked flask bile acid (5 mmol, 1 eq.) and 1,4-dioxane (42 mL) were cooled on an ice-water bath to +10 ºC. To the cooled solution triethyl amide (6.7 mmol, 1.34 eq.) was added from a dropping funnel, followed by a dropwise addition of ethyl chloroformate (6.7 mmol, 1.34 eq.) in 1,4-dioxane (3 mL). The mixture was stirred at rt for 30 min. Meanwhile in another flask ethyl amide hydrochloride (6.7 mmol, 1.34 eq.) was suspended in DMF (10 mL). Suspension was cooled on ice-salt bath to 0 ºC after which triethyl amide (7.4 mmol, 1.48 eq.) was added from a dropping funnel. The mixture was stirred at rt for 30 min. Ethyl amide in DMF was added dropwise to the bile acid anhydride and stirring of the reaction mixture continued at rt for 20 h. Volatiles were evaporated and the crude product was dissolved in $CHCl_3$ (100 mL). The crude product was washed with water (2×75 mL), 0.1 M HCl solution (2×75 mL), water (2×75 mL), and brine (2×75 mL). The organic layer was dried (Na_2SO_4), filtered, and the volatiles evaporated under reduced pressure. The crude products were purified by column chromatography (silica gel, DCM:MeOH 96:4 for **1**, 90:10 for **2**, x:y for **4**, and $CHCl_3$:MeOH 86:14 for **3**). All pure products were dried under vacuum.

2.2.1 Lithocholic acid ethyl amide **1**

Yield 57 %. ^{1}H NMR ($CDCl_3$, 500 MHz, ppm): δ 5.44 (t, 1H, NH), 3.62 (m, 1H, 3β-H), 3.28 (m, 2H, 25-CH_2), 2.21/2.04 (m, 2H, 23-CH_2), 1.14 (t, 3H, 26-CH_3), 0.91 (d, 3H, 21-CH_3), 0.91 (s, 3H, 19-CH_3), 0.64 (s, 3H, 18-CH_3). ^{13}C NMR ($CDCl_3$, 126 MHz, ppm): δ 173.4 (C-24), 71.8 (C-3), 56.5 (C-14), 56.1 (C-17), 42.8 (C-13), 42.1 (C-5), 40.5 (C-9), 40.2 (C-12), 36.5 (C-4), 35.9 (C-8), 35.5 (C-20), 35.4 (C-1), 34.6 (C-10), 34.3 (C-25), 33.7 (C-23), 31.8 (C-22), 30.6 (C-2), 28.2 (C-16), 27.2 (C-6), 26.4 (C-4), 24.2 (C-15), 23.4 (C-21), 20.8 (C-7), 18.4 (C-19), 14.9 (C-26), 12.0 (C-18). MS: *m/z* 426.7 $[M+Na]^+$, 830.5 $[2M+Na]^+$.

2.2.2 Deoxycholic acid ethyl amide **2**

Yield 75 %. ^{1}H NMR ($CDCl_3$, 500 MHz, ppm): δ 5.50 (t, 1H, NH), 3.97 (m, 1H, 12β-H), 3.61 (m, 1H, 3β-H), 3.28 (m, 2H, 25-CH_2), 2.23/2.06 (m, 2H, 23-CH_2), 0.97 (d, 3H, 21-CH_3), 0.90 (s, 3H, 19-CH_3), 0.65 (s, 3H, 18-CH_3). ^{13}C NMR ($CDCl_3$, 126 MHz, ppm): δ 173.4 (C-24), 73.2 (C-12), 71.8 (C-3), 48.3 (C-14), 47.2 (C-17), 46.5 (C-13), 42.1 (C-5), 36.4 (C-4), 36.0 (C-8),

35.2 (C-1, C-20), 34.4 (C-25), 34.1 (C-10), 33.7 (C-9), 33.5 (C-23), 31.7 (C-22), 30.5 (C-2), 28.7 (C-11), 27.5 (C-16), 27.1 (C-6), 26.1 (C-7), 23.7 (C-15), 23.2 (C-19), 17.5 (C-21), 14.9 (C-26), 12.8 (C-18). MS: *m/z* 442.7 $[M+Na]^+$, 862.5 $[2M+Na]^+$.

2.2.3 Cholic acid ethyl amide **3**

Yield 53 %. ^{1}H NMR ($CDCl_3$, 500 MHz, ppm): δ 5.76 (t, 1H, NH), 3.96 (m, 1H, 12β-H), 3.84 (m, 1H, 7β-H), 3.44 (m, 1H, 3β-H), 3.27 (m, 2H, 25-CH_2), 2.21/2.09 (m, 2H, 23-CH_2), 0.99 (d, 3H, 21-CH_3), 0.88 (s, 3H, 19-CH_3), 0.68 (s, 3H, 18-CH_3). ^{13}C NMR ($CDCl_3$, 126 MHz, ppm): δ 173.6 (C-24), 73.1 (C-12), 72.0 (C-3), 68.4 (C-7), 46.8 (C-17), 46.5 (C-13), 41.9 (C-14), 41.5 (C-5), 39.7 (C-4), 39.6 (C-8), 35.3 (C-1, C-20), 34.7 (C-6, C-10), 34.4 (C-23), 33.3 (C-25), 31.7 (C-22), 30.6 (C-2), 28.3 (C-11), 27.5 (C-16), 26.6 (C-9), 23.2 (C-15), 22.5 (C-19), 17.5 (C-21), 14.9 (C-26), 12.6 (C-18). MS: *m/z* 458.8 $[M+Na]^+$, 474.8 $[M+K]^+$, 894.6 $[2M+Na]^+$.

2.2.4 Dehydrocholic acid ethyl amide **4**

Yield 34 %. ^{1}H NMR ($CDCl_3$, 500 MHz, ppm): δ 5.50 (t, 1H, NH), 3.27 (m, 2H, 25-CH_2), 2.88 (m, 1H, 8-CH), 1.39 (t, 3H, 26-CH_3), 1.12 (d, 3H, 21-CH_3), 1.06 (s, 3H, 19-CH_3), 0.84 (s, 3H, 18-CH_3). ^{13}C NMR ($CDCl_3$, 126 MHz, ppm): δ 211.9 (C-12), 208.9 (C-3), 208.6 (C-7), 173.1 (C-24), 56.9 (C-13), 51.8 (C-14), 48.9 (C-8), 46.8 (C-5), 45.6 (C-17), 45.5 (C-9), 44.9 (C-6), 42.8 (C-4), 38.6 (C-11), 36.4 (C-2), 35.9 (C-10), 35.5 (C-20), 35.2 (C-1), 34.3 (C-25), 33.6 (C-23), 31.2 (C-22), 27.6 (C-15/C-16), 25.1 (C-15/C-16), 21.9 (C-26), 18.7 (C-18), 14.9 (C-21), 11.8 (C-19). MS: *m/z* 452.7 $[M+Na]^+$, 484.8 $[M+MeOH+Na]^+$.

2.3 NMR spectroscopy

^{1}H, ^{13}C, and 2D ^{1}H, ^{13}C HMQC and HMBC spectra used for characterization of the compounds **1**–**4** were recorded with a Bruker Avance DRX 500 MHz spectrometer. The spectrometer was equipped with 5 mm diameter broad band inverse detection probehead operating at 500.17 MHz in ^{1}H and 125.77 MHz in ^{13}C experiments, respectively. The ^{1}H NMR chemical shifts are referenced to the signal of residual $CHCl_3$ (7.26 ppm from internal TMS). The ^{13}C NMR chemical shifts are

referenced to the centre peak of the solvent $CDCl_3$ (77.0 ppm from internal TMS). A composite pulse decoupling, Waltz-16, has been used to remove proton couplings from ^{13}C NMR spectra.

2.4 Mass spectrometry

Compounds **1**–**4** were studied by mass spectrometry. Measurements were performed by using Micromass LCT time of flight (TOF) mass spectrometer with electrospray ionization (ESI). Measurements were conducted using positive ion mode. MassLynx NT software system was used to control the spectrometer, and to acquire and process the data. Flow rate for the sample solutions was 10 µL/min. Sample cone and extraction cone potentials were 40 V and 6 V, respectively. The capillar cone potential varied between 3600 V and 4000 V, RF lens potential was 250 V in all measurements. The desolvation temperature was set to 120 °C and the source temperature to 80 °C.

Stock solutions of compounds **1**–**4** were 1 mM in acetone. Measurement solutions were prepared from stock solutions by diluting them to 10 µM or 20 µM in methanol.

2.5 IR-spectroscopy

Compounds **1**–**4** were studied by IR-spectroscopy. Measurements were conducted using Bruker Tensor 27 Fourier transform IR-spectrometer equipped with GladiATR™ accessory in the range of 400–4000 cm^{-1}. Compounds **1**–**4** were measured in solid state. Hydrogels formed by compound **1** in 2 % (w/v) in 50:50 H_2O:2-propanol, and 10:90 H_2O:acetone and H_2O:acetonitrile were also studied. For the measurements of the hydrogels of compound **1**, the solution system in question was measured and the spectrum obtained was subtracted from the spectrum of the gel to eliminate the background signal.

2.6 Gelation studies

Self-assembly properties of compounds **1**–**4** were studied by weighing 5 mg to obtain 1 % (w/v) systems or 10 mg to obtain 2 % (w/v) systems of a particular compound in a test tube and adding 500 µl of solvent or solvent mixture in question. The mixture was subjected to ultrasound for ca. 1 min with the cap on and heated with a heat gun until the compound was dissolved or the boiling point of the solvent reached without the cap. The solution or suspension was cooled to rt and the

observations with regard gelation were made within 1-2 h after cooling had commenced. Formed solid mass was defined as a gel if there was no solvent flow when test tube was inverted. Possible crystallization and precipitation was observed within days or weeks. Test tubes were stored at rt during the observation time.

2.7 SEM

Samples for SEM were prepared by a traditional method. The hot solution containing the gelator in question in an appropriate solvent system was pipetted to the sample stub, and the gel allowed to form while cooling to room temperature. In addition to the traditional method, samples were prepared also directly from previously formed gels. A small amount of a gel in question was scooped with a spatula and the sample stub was thinly brushed with the gel. The gel was allowed to dry on the sample stub in both methods of sample preparation. After drying, all samples were thinly plated with gold with JOEL Fine Coat Ion Sputter JFC-1100. Micrographs were taken with Bruker Quantax400 EDS scanning electron microscope equipped with a digital camera.

2.8 Toxicity evaluation

2.8.1 Cell culture

Mouse fibroblasts Balb/c 3T3 (No. 86110401) was obtained from European Collection of Cell Cultures (UK). Cell line stored in a cryovial were taken out of the liquid nitrogen and thawed in water (25 °C; 1 min). Using a pipette, cells were transferred into a 25 cm^2 tissue culture flask containing 10 ml of pre-heated culture medium (DMEM, penicillin 100 U/ml, L-glutamine 2 mmol/l, streptomycin 100 mg/l, fetal calf serum 5%, new born calf serum 5%) and incubated in humidified atmosphere with 5 % (v/v) CO_2 at 37 °C. The medium was changed every 24-48 h. Cells were cultivated to approach confluence and were passaged. The medium was replaced and cells were washed with PBS (5 ml). Solution was removed and 0.25% trypsin-EDTA was added (0.5 ml, 2-3 min, 37 °C). Then 5 ml of culture medium was applied, cells were centrifuged (10 min; 1300 rpm; RT) and the supernatant was removed. The cell pellet was resuspended in 20 ml of culture medium and suspension was transferred to the 75 cm^2 cultivating flask. During cultivating in a 75 cm^2 tissue culture flask the procedure was the same, only 10 ml of PBS, 1 ml of trypsin-EDTA and 10 ml of culture medium were used.

2.8.2 Sample preparation

Stock solutions of samples **1** and **2** (0.039–5 mg/ml) and **3** and **4** (0.156–20 mg/ml) were prepared in DMSO. The final concentration of DMSO in serum-free medium was 0.5 % (v/v). The DMSO was added to the compounds, thoroughly mixed (2 min), and sonicated (10 min). Control cells were incubated with a corresponding volume of DMSO.

2.8.3 Procedure

The concentrations of the cells were determined using coloured with trypan blue. The cells were seeded in 96-well plates at a density of $0.8x10^5$ cells/ml (200 µl/well) in culture medium and incubated for 24 h in a humidified atmosphere (37 °C, 5 % CO_2). Then the culture medium was change to the serum-free one containing test compounds in concentration ranges of 0.195–25 µg/ml for **1** and **2**, and 0.781–100 µg/ml for **3** and **4**, and incubated for 24 h (37 °C, 5 % CO_2). After incubation period the cell damage was evaluated as the incorporation of neutral red into the lysosomes of living cells (Neutral red assay). The test was performed in 3 independent experiments.

2.8.4 Neutral red assay

The neutral red (NR) assay is grounded on the fact that live (non-damaged) cells intake and store NR into their lysosomes. The concentration of the incorporated dye is determined spectrophotometrically at 540 nm after extraction of retained NR into acidic methanolic solution.[42]

After the incubation period the cells were first washed with PBS, and subsequently NR solution (0.03%, w/v in PBS) was applied to the cells for 3 h (37 °C, 5 % CO_2). Then the cells were washed with a washing solution (formaldehyde (0.125%; v/v), $CaCl_2$ (0.25%, w/v)), and the retained NR was dissolved in extraction solution (methanol (50%; v/v), acetic acid (1%; v/v)). The absorbance was measured with a microplate reader (Sunrise Remote, Tecan, Austria).

2.9 X-ray crystallography

Single crystal X-ray data for **1**, **2**, and **3** were collected at either 120 or 123 K using Agilent Super-Nova dual source wavelength diffractometer with an Atlas CCD detector using multilayer optics monochromatized CuK_α (λ = 1.54184 Å) radiation. The data collection and reduction for **1**, **2**, and **3** was performed using the program *CrysAlisPro*.[43] Gaussian face index absorption correction method[43] was used for **1**, **2**, and **3**. All the structures were solved with direct methods (*SHELXS)*[44] and refined by full-matrix least squares on F^2 using the *OLEX2*[45], which utilizes the *SHELXL*-2013 module.[44] No attempt was made to locate the hydrogens for solvent molecules and heteroatoms, and all the hydrogen atoms were added using ADD H command in *OLEX2*. Attempts to solve the disorder of N-ethyl chain in compound **3** still engenders B-alerts and requires the usage of constraints (EADP) and restraints (ISOR), which ultimately affects the R_1-value significantly. As a result, considering the conformational importance of side chain during our discussion, no attempt was made to solve the disorder.

3. Results and discussion

3.1 Synthesis

A well-established method, employed several times by our research group[41,46], was used to synthesize compounds **1**–**4**. Syntheses were relatively fast compared to syntheses that last several days [46]. Purification of compounds **3** and **4** was challenging, probably due to the three hydrophilic functional groups of the steroidal backbone which cause stronger interactions with silica gel when using column chromatography. Yields varied between 34–75 %.

3.2 Gelation studies

Gelation properties of compounds **1**–**4** (figure 1) were tested in 28 solvents at 1 % (w/v) and in various aqueous solutions at 1 % and 2 % (w/v) concentration. The results obtained are summarized in Tables 1 and 2, respectively.

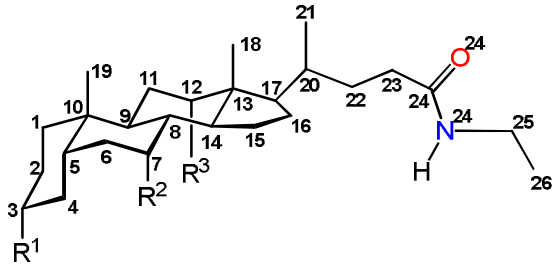

Figure 1: Chemical structures of compounds **1**–**4**.

Table 1: Gelation test results for compounds **1**–**4** at 1 % (w/v) concentration.

Solvent	**1**	**2**	**3**	**4**
$CHCl_3$	S+	S+, S	S+	S+
DCM	PS+, S	S+, S	PS+, S, P	S+
CCl_4	PS+, PS	PS+, PS	PS+, PS	PS+, PS
Benzene	PS+, PS, **G**	PS, S	PS+, PS	PS+, PS
Chlorobenzene	PS+, S, **G**	PS+, S	PS+, S	PS+, S
tert-Butylbezene	PS+, S	PS+, PS	PS+, S	PS+, S, P
Toluene	PS+, PS, **G**	PS+, S, PS	PS+, S	PS+, S
p-Xylene	PS+, S, **G**	PS+, S, PS	PS+, S	PS+, PS
m-Xylene	PS+, S, PG	PS+, S, PS	PS+, S	PS+, PS
o-Xylene	PS+, S, **G**	PS+, S, PS	PS+, S	PS+, S
Cumene	PS+, S	PS	PS+, S	PS+, PS
Mesitylene	PS+, S, PG	PS+, S, PS	PS+, S	PS+, S
Anisole	PS+, S, **G**[a]	PS+, S, PS	PS+, S	PS+, S
Cyclohexene	S+	PS+, S	S+	PS+, S, P
Ethylacetate	PS+, PS, PG	PS+, S	PS+, S, P	PS+, S
Hexane	PS+, PS	PS+, PS, P	PS+, PS	PS+, PS, P
Acetone	PS+, PS, **G**	PS+, S	PS+, S	PS+, S
ACN	PS+, PS, **G**	-	PS+, S	S+
DMF	PS+, S	S+, S	S+	S+
Acetic acid	S+	S+, S	S+	S+
THF	S+	S+, S	S+	PS+, S
MeOH	S+	S+, S	S+	PS+, S, P
EtOH	S+	S+, S	PS+, S	PS+, PS
2-Propanol	S+	S+, S	S+	PS+, PS
1-Butanol	S+	S+, S	S+	PS+, S, P
1-Octanol	S+	PS+, S	S+	PS+, S, P
Cyclohexanol	PS+, S	PS+, S	PS+, S	PS+, S
2 M HCl	PS+, PS, P	PS+, PS	PS+, PS	PS+, PS, P
Deionized H_2O	PS+, PS, P	PS+, PS, P	PS+, PS, P	S+
Pyridine	S+	S+, S	S+	PS+, PS

S+ = soluble without heating, S = soluble with heating, PS = partially soluble with heating, I = insoluble, G = gel with appr. 0–5 % free solvent, G- = gel with appr. 5–20 % free solvent, G[a] = gel formed after one day, PG = gel with appr. 50 % free solvent, P = precipitates on cooling.

Table 2: Gelation test results for compounds **1**–**4** at 1 % (w/v) concentration in aqueous solutions.

	1	**2**	**3**	**4**
50:50				
H_2O:MeOH	PS+, PS, P	PS+, S, P	PS+, PS	PS+, PS
H_2O:EtOH	PS, P	S	S	S
H_2O:acetone	PS, P	S	S	S
H_2O:ACN	PS, P	S, P	S	S, P
H_2O:2-propanol	PS, P, gel-like	S	S	S+
60:40				
H_2O:MeOH	PS+, PS, P	PS+, PS, P	PS+, S, PS	PS+, PS
H_2O:EtOH	PS, P	S, P	S	PS, P
70:30				
H_2O:MeOH	PS+, PS, **G**	PS+, PS, suspension	PS+, PS, S	PS+, PS
H_2O:EtOH	PS, P	PS, P	S+, P	PS, P
80:20				
H_2O:EtOH	PS, P	S+, P	PS, P	PS, P
10:90				
H_2O:EtOH	S+	S+	S+	S+
H_2O:acetone	S, **G-**	S+	S	S
H_2O:ACN	S+, P, gel-like	S	S	S
H_2O:2-propanol	S+	S+	S	S+
20:80				
H_2O:EtOH	S	S+	S+	S+
30:70				
H_2O:EtOH	S+	S	S	S+
H_2O:acetone	PS, P	S	S	S
H_2O:ACN	PS, P	S	S	S+, P
H_2O:2-propanol	S	S	S	S+

S+ = soluble without heating, S = soluble with heating, PS = partially soluble with heating, I = insoluble, G = gel with appr. 0–5 % free solvent, G- = gel with appr. 5–20 % free solvent, G[a] = gel formed after one day, P = precipitates on cooling.

A total of 19 gel systems were obtained, most of which in aromatic solvents. Five of the obtained gel systems were partial gels. Aromatic solvents included benzene, chlorobenzene, *tert*-butylbenzene, toluene, *p*- and *o*-xylene, and anisole. Compound **1** formed gels in acetone and acetonitrile in addition to aromatic solvents. Partial gels of compound **1** formed in *m*-xylene, mesitylene, and ethylacetate. Compound **4** formed 2 % (w/v) gel in ethanol and a 2 % (w/v) weak gel in 2-propanol. Lithocholic acid derivative **1** formed the majority of the gel systems, a total of 16 gel systems, which is common for bile acid derivatives. For example, most of the gel systems from the bile acid cysteamine and alkylamide derivatives reported previously by our research group tended to be formed by lithocholic acid derivatives [37,38]. Some of the gel systems in previous studies were obtained with dehydrocholic acid derivatives, as well [35].

In the present study we found that lithocholic acid derivative **1** had interesting properties in water solutions. The solution systems for 1 % (w/v) hydrogelation tests were selected based on the gel systems obtained in organogelation tests. Furthermore, the solution systems for 2 % (w/v) hydrogelation tests were chosen based on results from previously conducted 1 % (w/v) hydrogelation tests. Compound **1** generated five hydrogel systems, of which three were strong gels. The 1 % (w/v) weak gel by compound **1** formed in 10:90 H_2O:acetone. Two of the three strong gels by compound **1** formed as 2 % (w/v) in 50:50 H_2O:2-propanol and 10:90 H_2O:acetonitrile. One strong gel formed as 1 % (w/v) in 70:30 H_2O:MeOH. Compound **1** also formed a partial gel as 2 % (w/v) in 10:90 H_2O:acetone. In addition to actual gel systems, compound **1** formed gel-like systems as 1 % (w/v) in 50:50 H_2O:2-propanol and 10:90 H_2O:acetonitrile. Compound **2** was found to create partial gel as 2 % (w/v) in 70:30 H_2O:MeOH. Interestingly, the three proper hydrogels disintegrated instantly when disturbed with a spatula making them thixotropic by nature. The same phenomenon was observed for compound **1** 1 % (w/v) gel in acetonitrile when preparing the SEM samples.

3.3 IR

The IR spectra of the solid compounds **1**–**4** were very similar with each other showing just a little variation in the amide bond's carbonyl stretching mode (Table 3). The solid compound **1** and the

2 % hydrogels (50:50 H_2O:2-propanol, 10:90 H_2O:acetone and H_2O:acetonitrile) of compound **1** were rather uniform when compared to each other. In the spectrum of 2 % (w/v) hydrogel of compound **1** in 10:90 H_2O:acetone, however, a broad band at 3300–3500 cm^{-1} was observed (Figure 2), probably due to hydrogen bonding of the gelator molecules. Since, based on X-ray crystallography, hydrogen bonding is important in stabilizing the solid state structures, and since the difference to the spectrum of solid compound **1** is so small, hydrogen bonding in not necessarily the only driving force in the gel network formation.

Table 3: Selected IR bands for compounds **1**–**4** and hydrogels of compound **1**.

Sample	Amide I (cm^{-1})	Amide II (cm^{-1})	Amide B (cm^{-1})	vNH/OH (cm^{-1})
1	1655	1546	2932	3325, 3432
2	1624	1530	2926	3369
3	1612	1557	2927	3281,3419, 3511
4	1701	1543	2970	3287, 3391
2% **1** in 50:50 H_2O:2-propanol	1655	1545	2932	3322, 3431
2 % **1** in 10:90 H_2O:acetone	1655	1545	2932	3326, 3435
2 % **1** in 10:90 H_2O:acetonitrile	1655	1545	2932	3324, 3434

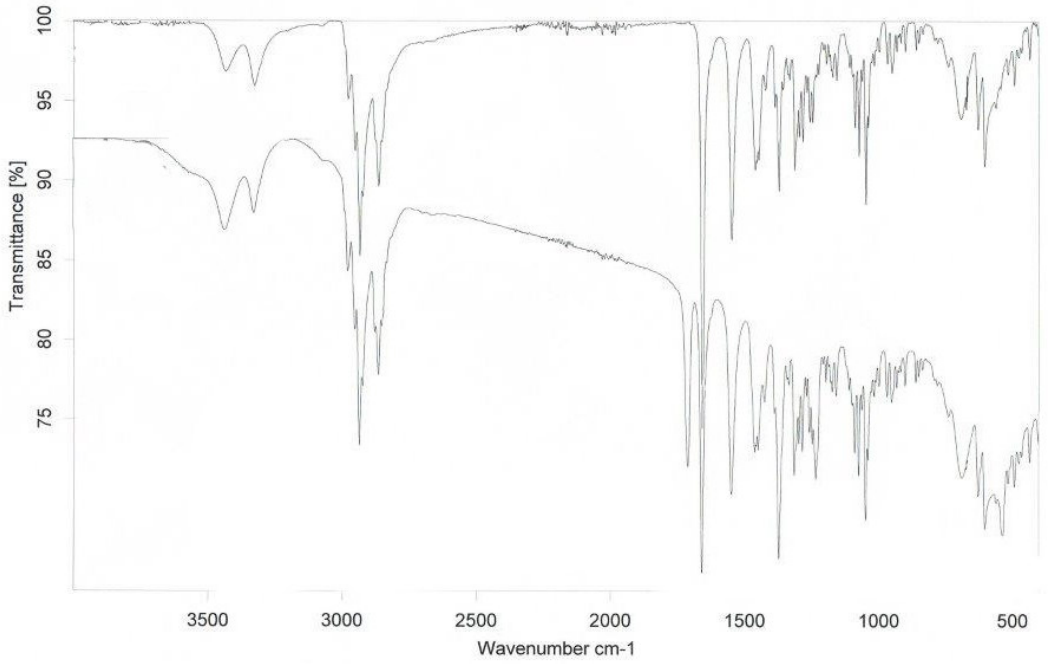

Figure 2: IR spectra of compound **1** (above) and 2 % (w/v) gel of compound **1** in 10:90 H2O:acetone (below).

3.4 Microscopy

The hydrogels formed by compound **1** were studied with scanning electron microscope (SEM). When comparing the SEM images of gels formed by compound **1** in aqueous solutions, it was found that the self-assembly patterns diverge from each other depending on the method of sample preparation. In the case of samples prepared from hot solutions, gel fibers resembled stalks of grass. However, gelator molecules appeared to form spherical assemblies consisting of fiber bundles resembling old fashioned dusters in samples prepared from gels directly. The assemblies of these bundles were a spitting image of dandelions fluffy seeds. This was most clearly seen in images of the 2 % (w/v) gel of compound **1** in 50:50 H_2O:2-propanol (Figure 3).

In all the gels studied the fiber sizes were similar. Straight fibers in samples prepared from hot solutions varied in width between 1–15 µm and in length between 20–240 µm. In samples prepared by scooping a portion of the gel on the sample stub single fibers were similar in width compared to stalk like fibers. However, the single fibers were longer, the length varied between 60–410 µm. The diameter of the spherical assemblies varied between 390–740 µm.

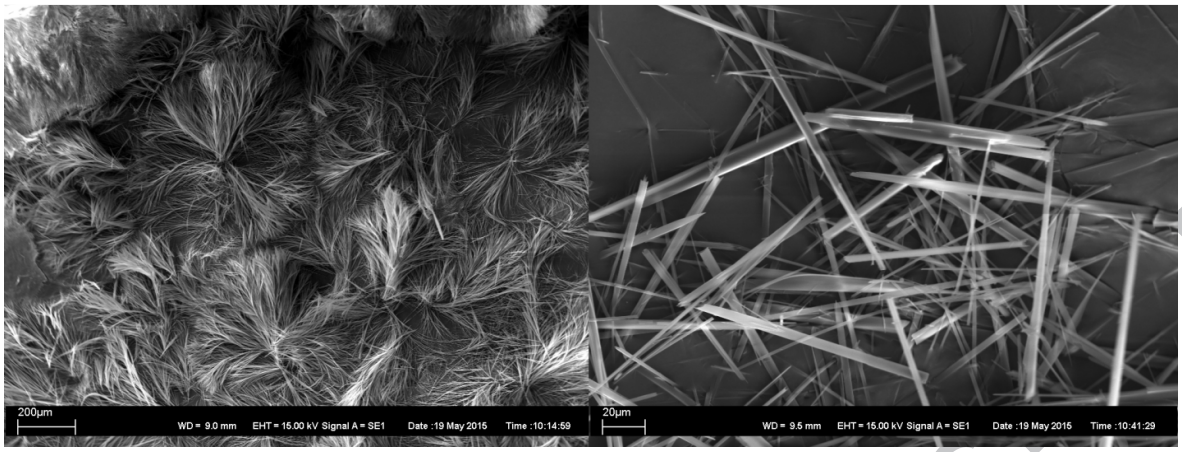

Figure 3: 2 % (w/v) gel of compound **1** in 50:50 H_2O:2-propanol. Sample prepared from gel (left) and sample prepared from hot solution (right).

3.5 Results of the neutral red assay

The standard mouse cell line Balb/c 3T3, commonly used in accredited tests, was used for the toxicity study. The neutral red (NR) assay was performed for compounds **1**-**4** (see Equation E1 and Figures S1-S4). It is based on the fact that live (non-damaged) cells intake and store NR into their lysosomes, and the concentration of the incorporated dye can then be determined spectrophotometrically. The toxicity data are expressed as IC_{50} ± S.D. (µg/ml) values. Substances efficiency in inhibiting specific biochemical or biological function is described as the half maximal inhibitory concentration (IC_{50}). As can be seen from Table 4, the highest cell viability in the series of compounds was shown by compound **3**, which did not form any gels. Compound **1**, which formed hydrogels, showed third lowest toxicity in the series. In a previous study performed by us for bile acid-cysteamine conjugates [35] it was observed that the hydroxyl group in position 7α and/or 12α might cause the compound to show toxicity, whereas the non-toxic compounds only had a 3α-hydroxyl, 3α- and 7β-hydroxyls, or no hydroxyl groups at all. The current results don't agree with those hypotheses, even though compound **4** bearing no hydroxyls shows the second lowest toxicity in the series.

Table 4: Toxicity of tested compounds evaluated using NR assay.

Compounds	Concentration range (µg/ml)	IC_{50} ± S.D. (µg/ml)
1	0.2-25	22.70 ± 2.16
2	0.2-25	12.31 ± 2.08
3	0.8-100	73.50 ± 4.58
4	0.8-100	* 65.17 ± 3.30

***** Cell viability evaluated at the highest concentration express as % of control

3.6 X-ray crystallography

Despite many bile acid crystal structures have characteristic bilayer hydrogen bonding, the position and number of hydroxyl groups on the amphiphilic face play an important role to form a variety of hydrogen bonded supramolecular networks. These robust facial amphiphiles with different number of hydroxyl groups are carefully engineered for different applications *e.g.* micellar and interactions with biological membranes.[47–49] Another appealing solid-state property, which leads to remarkable lattice stabilization patterns, is their side chain modification. Modifications of side chains in bile acids have been extensively reviewed[50-54] and unarguably the conformations adopted by side-chains has represented wide range of applications in the field of crystal engineering, co-crystals, improved biological activity, and pharmaceutical applications. In the current study, inspired by the gelation properties, single crystals of *N*-ethylamide derivatives of lithocholic acid (**1**), deoxycholic acid (**2**) and cholic acid (**3**) were grown from acetonitrile by solvent evaporation to study the effect of inclusion of amide functionality to the hydrogen bonded bilayers.

Compound **1** crystallized in the monoclinic space group $P2_1$ with one molecule in the asymmetric unit. As can be seen from Figure 4a the peripheral hydroxyl group at 3α-position and the *N*-alkylamide side chain with *tttt* conformation[55] are orientated in the same direction. As a result, the hydroxyl group at 3α-position as well as the carbonyl and N-H groups in the side-chain drive **1** to give infinite one-dimensional bilayers stabilized by O-H•••O [*d*(O•••O), 2.857(3) Å] and N-H•••O

[*d*(N•••O), 3.083(3) Å] interactions (Figure 4b). Compound **2**, however, crystallized in the triclinic space group *P*-1 containing three crystallographically independent molecules of **2** (see Table S1) and four acetonitrile molecules in the asymmetric unit. The dihedral angles C13-C17-C20-C22, C17-C20-C22-C23, C20-C22-C23-C24, and C22-C23-C24-N24 (Table 5) for all the three molecules in the asymmetric unit are close to *ttgt* conformations. The hydroxyl groups at 12α-positions, the carbonyl oxygens, and the N-H groups form intermolecular O-H•••O and N-H•••O hydrogen bonds while the peripheral hydroxyl groups at 3α-positions hydrogen bonds to acetonitrile molecules (Figure 4c). Although the molecule has features to crystallize in high symmetry space groups with screw axes, the hydroxyl groups at 12α-position and the fourth acetonitrile molecule presumably destroy the symmetry to bring molecules closer to form O-H•••O and N-H•••O interactions giving **2** wriggly motifs. The intermolecular hydrogen bond between the three bile acid molecules contributes to the induction of a 1-D columnar type assembly, possessing analogous features of helices, as shown in Figure 4d. A perspective view of the crystal packing in **2** suggests that the self-organization in bile acids is dependent on positions of the hydroxyl groups and on the side chain conformations.

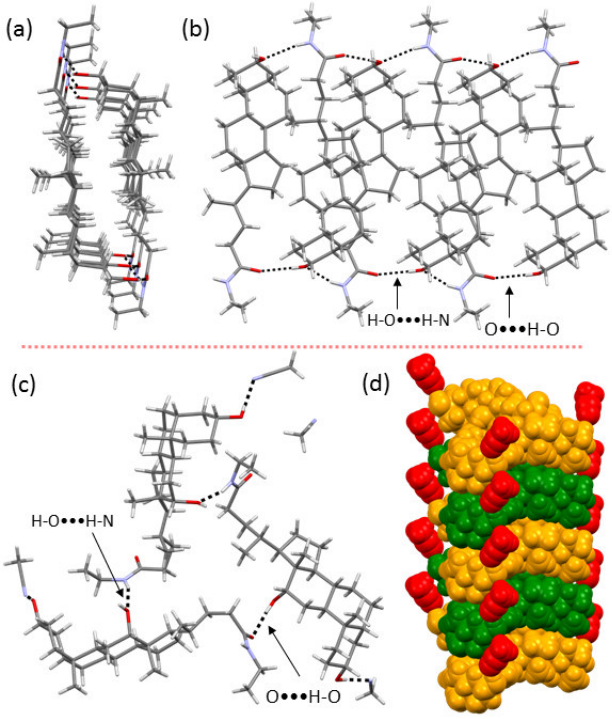

Figure 4. (a) 1-D Polymeric structure of **1**, and (b) side-view to show 3α-hydroxyl group and *N*-ethylamide chain orientation in capped stick model. (c) Top-view of 1-D hydrogen bonded trimeric

structure of **2** in capped stick model. (d) Side-view to stacking arrangement of trimers in **2** in CPK model. Representation: Orange and green - compound **2**, and red - acetonitrile. Black broken lines represent hydrogen bonding.

Compound **3** crystallized in the monoclinic space group *C*2, the asymmetric unit containing two crystallographically independent molecules of **3** and an acetonitrile molecule. The structural difference in the side chains with *tgtg* and *tttt* conformations, and the intermolecular N-H•••O connectivity resulted in twice the unit cell *a*-axis length of **1**, as shown in Figure 5a. The side chain with the *tgtg* conformation carrying an N-H group, and the hydroxyl groups of amphiphilic face of compound **3** give a bilayer structure by O-H•••O and O-H•••O interactions. On the other hand, the side chain with *tttt* conformation carrying the N-H group hydrogen bonds directly to an acetonitrile molecule as shown in Figure 5b.

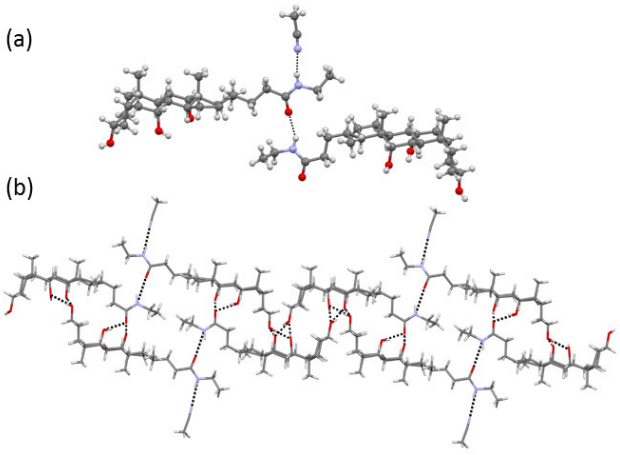

Figure 5. (a) Asymmetric unit of **3** in ball and stick model, and (b) section of crystal packing to show bilayer formation (capped stick model). Hydrogen and solvent molecules are omitted for clarity. Black broken lines represent hydrogen bonding.

Table 5: Dihedral angles of the side-chains (°) of **1**, **2**, and **3**.

	1	**2**	**3**
C13-C17-C20-C22	174.3(2)	-174.0(2)	175.3(3) [169.5(3)]
C17-C20-C22-C23	-173.5(2)	-174.0(2)	59.4(4) [-156.9(3)]
C20-C22-C23-C24	172.6(2)	72.3(3)	178.9(3) [-163.8(4)]
C22-C23-C24-N24	136.3(2)	-125.9(3)	-3.6(5) [-155.0(4)]

The bilayered structures formed by O-H•••O interactions are robust, and the structural rigidity gives the lipophilic faces a characteristic corrugated property. The repulsion between methyl groups in the crystal packing makes the lipophilic face offset stabilized by hydrogen bonding and van der Waals interactions. As a result, based on the interdigitation of C18 and C19 methyl groups in lipophilic face and two possible conformations of the side chain, the host frameworks in these crystal structures were classified into four types; *α-gauche, β-trans, β-gauche*, and *α-trans*.[56] The side chain dihedral angle (C17-C20-C22-C23) is generally used to distinguish the four types. The side chain with *tgtg* conformation has dihedral angle (C17-C20-C22-C23) of 59.4(4)°, which corresponds to *α-gauche* type, whereas the interdigitation of methyl group suggests the host-framework being of *β-gauche* type. On the other hand, the side chain with *tttt* conformation has a dihedral angle (C17-C20-C22-C23) of -156.9(3)°, in which the stacking associates uniquely to *α-trans* type, as shown in Fig 6. To the best of our knowledge, two host framework arrangements identified within a crystal packing has not been previously reported.

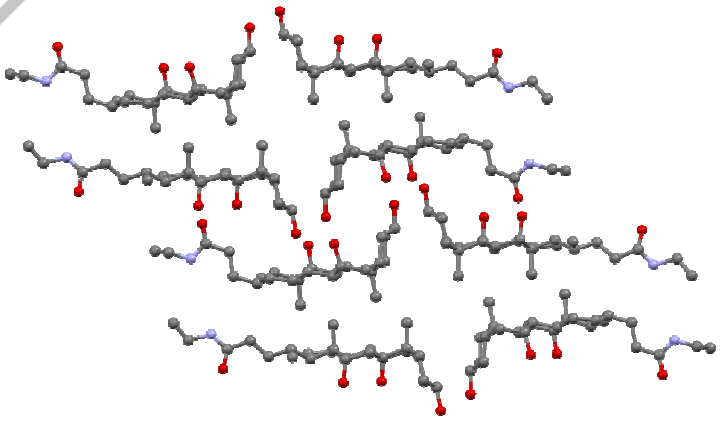

Figure 6: Section of crystal packing viewed along *b*-axis to show *α-gauche* and *α-trans* type host arrangements in **3**, in ball and stick model. Hydrogen and solvent molecules are omitted for clarity.

During crystallizations, most bile acids prefer anhydrous form due to bilayered O-H•••O interactions, and thus can adopt significant conformational changes for side chains in co-crystals. Bile acids without hydroxyl groups are often and sometimes difficult to crystallize. For example in the current study, attempts to obtain good quality crystals of compound **4** were unsuccessful. Thin needle shape crystals were obtained after boiling **4** overnight in 1:1 water:methanol solvent ratio (data completeness < IUCr limit). However, the crystal structure shows that the lattice stabilization occurs uniquely at N-H functional group with methanol and water molecules.

Crystal data and X-ray experimental details for compounds **1**, **2**, and **3** are presented in Table S2.

4. Conclusions

As a continuation of the series of bile acid alkyl or functionalized alkyl amide/ester derivatives capable of acting as gelators, in this work four new bile acid ethyl amide derivatives were synthesized and characterized in detail. Gelation experiments for the synthesized molecules resulted in a total of 19 gel systems, most of which in aromatic solvents. Lithocholic acid derivative **1** formed the majority of the gel systems, which is common for bile acid derivatives. Furthermore, compound **1** generated five hydrogel systems, which showed thixotropic nature. For the best of our knowledge, this is the first time when supramolecular hydrogels involving bile acid alkyl amides is reported. The properties of the hydrogels were investigated using SEM and IR spectroscopy, and the toxicity of the compounds determined. Solid state packing of compounds **1**-**3** was defined by using single crystal X-ray crystallography. The packing patterns may provide an idea about the gel state assembly of the molecules, eventually shedding light to the phenomena underlying gel formation.

Bile acid-based hydrogels have potential use in biological applications both because they form in biocompatible solvents and because they are formed by nontoxic endogenous gelators. The biocompatibility of a hydrogel provides perhaps new potential applications regarding biomedicine, such as drug delivery, artificial tissue engineering, etc.

Acknowledgements

Ellen and Artturi Nyysönen Foundation (R.K.) is acknowledged for financial support. The authors are grateful to Lab. Eng. E. Haapaniemi for NMR spectroscopy measurements and Lab. Tech. H. Salo for SEM studies.

References

1 A. F. Hofmann and L. R. Hagey, *Cell. Mol. Life Sci.*, 2008, **65**, 2461–83.

2 M. J. Monte, J. J. G. Marin, A. Antelo and J. Vazquez-Tato, *World J. Gastroenterol.*, 2009, **15**, 804–16.

3 S. Mukhopadhyay and U. Maitra, *Curr. Sci.*, 2004.

4 A. F. Hofmann, *News Physiol Sci*, 1999, **14**, 24–29.

5 E. Virtanen and E. Kolehmainen, *European J. Org. Chem.*, 2004, **2004**, 3385–3399.

6 Shamsuzzaman, H. Khanam, A. Mashrai, A. Sherwani, M. Owais and N. Siddiqui, *Steroids*, 2013, **78**, 1263–1272.

7 K. H. Min, K. Park, Y. S. Kim, S. M. Bae, S. Lee, H. G. Jo, R. W. Park, I. S. Kim, S. Y. Jeong, K. Kim and I. C. Kwon, *J. Control. Release*, 2008, **127**, 208–218.

8 D.-H. Kim and A. C. Larson, *Biomaterials*, 2015, **56**, 154–164.

9 E. Im, S.-H. Choi, H. Suh, Y. H. Choi, Y. H. Yoo and N. D. Kim, *Cancer Lett.*, 2005, **229**, 49–57.

10 E. Im, Y. H. Choi, K.-J. Paik, H. Suh, Y. Jin, K.-W. Kim, Y. H. Yoo and N. D. Kim, *Cancer Lett.*, 2001, **163**, 83–93.

11 O. Briz, *Mol. Pharmacol.*, 2003, **63**, 742–750.

12 C. Valenta, E. Nowack and a Bernkop-Schnürch, *Int. J. Pharm.*, 1999, **185**, 103–111.

13 W. Kramer, G. Wess, A. Enhsen, E. Falk, A. Hoffmann, G. Neckermann, G. Schubert and M. Urmann, *J. Control. Release*, 1997, **46**, 17–30.

14 L. Galantini, M. C. di Gregorio, M. Gubitosi, L. Travaglini, J. V. Tato, A. Jover, F. Meijide, V. H. Soto Tellini and N. V. Pavel, *Curr. Opin. Colloid Interface Sci.*, 2015.

15 T. A. Al-Hilal, J. Park, F. Alam, S. W. Chung, J. W. Park, K. Kim, I. C. Kwon, I.-S. Kim, S. Y. Kim and Y. Byun, *J. Control. Release*, 2014, **175**, 17–24.

16 X.-Y. Jin, S.-Y. Fan, H.-W. Li, W.-G. Shi, W. Chen, H.-F. Wang and B.-H. Zhong, *Chinese Chem. Lett.*, 2014, **25**, 787–790.

17 E. Sievänen, *Molecules*, 2007, **12**, 1859–1889.

18 S. Y. Chae, S. Son, M. Lee, M. K. Jang and J. W. Nah, *J. Control. Release*, 2005, **109**, 330–344.

19 H. H. Moon, M. K. Joo, H. Mok, M. Lee, K. C. Hwang, S. W. Kim, J. H. Jeong, D. Choi and S. H. Kim, *Biomaterials*, 2014, **35**, 1744–1754.

20 D. Kim, D. Lee, Y. L. Jang, S. Y. Chae, D. Choi, J. H. Jeong and S. H. Kim, *Eur. J. Pharm. Biopharm.*, 2012, **81**, 14–23.

21 L. Mrózek, L. Dvořáková, Z. Mandelová, L. Rárová, A. Řezáčová, L. Plaček, R. Opatřilová, J. Dohnal, O. Paleta, V. Král, P. Drašar and J. Jampílek, *Steroids*, 2011, **76**, 1082–1097.

22 L. Coufalová, L. Mrózek, L. Rárová, L. Plaček, R. Opatřilová, J. Dohnal, K. Král'Ová, O. Paleta, V. Král, P. Drašar and J. Jampílek, *Steroids*, 2013, **78**, 435–453.

23 S. Banerjee, R. K. Das and U. Maitra, *J. Mater. Chem.*, 2009, **19**, 6649.

24 A. R. Hirst, B. Escuder, J. F. Miravet and D. K. Smith, *Angew. Chem. Int. Ed. Engl.*, 2008, **47**, 8002–18.

25 E. Caló and V. V. Khutoryanskiy, *Eur. Polym. J.*, 2014, **65**, 252–267.

26 P. Lee and M. A. Rogers, *Langmuir*, 2013, **29**, 5617–21.

27 L. Yan, G. Li, Z. Ye, F. Tian and S. Zhang, *Chem. Commun. (Camb).*, 2014, **50**, 14839–42.

28 J. W. Steed, *Chem. Commun. (Camb).*, 2011, **47**, 1379–83.

29 S. B. Schryver, *Proc. R. Soc. B Biol. Sci.*, 1914, **87**, 366–374.

30 S. B. Schryver, *Proc. R. Soc. B Biol. Sci.*, 1916, **89**, 176–183.

31 S. B. Schryver, *Proc. R. Soc. London. Ser. B, Contain. Pap. a Biol. Character*, 1916, **89**, 361–372.

32 M. R. Saboktakin and R. M. Tabatabaei, *Int. J. Biol. Macromol.*, 2015, **75**, 426–436.

33 V. Noponen, K. Toikkanen, E. Kalenius, R. Kuosmanen, H. Salo and E. Sievänen, *Steroids*, 2015, **97**, 54–61.

34 V. Noponen, A. Valkonen, M. Lahtinen, H. Salo and E. Sievänen, *Supramol. Chem.*, 2013, **25**, 133–145.

35 V. Noponen, H. Belt, M. Lahtinen, A. Valkonen, H. Salo, J. Ulrichová, A. Galandáková and E. Sievänen, *Steroids*, 2012, **77**, 193–203.

36 V. Noponen, S. Bhat, E. Sievänen and E. Kolehmainen, *Mater. Sci. Eng. C*, 2008, **28**, 1144–1148.

37 V. Noponen, M. Lahtinen, A. Valkonen, H. Salo, E. Kolehmainen and E. Sievänen, *Soft Matter*, 2010, **6**, 3789.

38 M. Löfman, J. Koivukorpi, V. Noponen, H. Salo and E. Sievänen, *J. Colloid Interface Sci.*, 2011, **360**, 633–44.

39 M. Löfman, M. Lahtinen, M. Pettersson and E. Sievänen, *Colloids Surfaces A Physicochem. Eng. Asp.*, 2015, **474**, 18–28.

40 M. Löfman, M. Lahtinen, K. Rissanen and E. Sievänen, *J. Colloid Interface Sci.*, 2015, **438**, 77–86.

41 E. Virtanen, J. Tamminen, J. Linnanto, P. Mätttäri, P. Vainiotalo and E. Kolehmainen, *J. Incl. Phenom. Macrocycl. Chem.*, **43**, 319–327.

42 I. G. . Maines, M.D.; Costa, L.G.; Reed, D.J.; Sassa, S.; Sipes, *Current protocols in toxicology*, John Wiley & Sons, New York, 1998.

43 *CrysAlisPro 2012, Agil. Technol. Version 1.171.36.35.*

44 G. M. Sheldrick, *Acta Crystallogr. A.*, 2008, **64**, 112–22.

45 O. V. Dolomanov, L. J. Bourhis, R. J. Gildea, J. A. K. Howard and H. Puschmann, *J. Appl. Crystallogr.*, 2009, **42**, 339–341.

46 A. Valkonen, M. Lahtinen, E. Virtanen, S. Kaikkonen and E. Kolehmainen, *Biosens. Bioelectron.*, 2004, **20**, 1233–41.

47 A. F. . Hofmann and B. . Borgström, *J. Clin. Invest.*, 1964, **43**, 247–57.

48 K. M. Giacomini, S.-M. Huang, D. J. Tweedie, L. Z. Benet, K. L. R. Brouwer, X. Chu, A. Dahlin, R. Evers, V. Fischer, K. M. Hillgren, K. A. Hoffmaster, T. Ishikawa, D. Keppler, R. B. Kim, C. A. Lee, M. Niemi, J. W. Polli, Y. Sugiyama, P. W. Swaan, J. A. Ware, S. H. Wright, S. W. Yee, M. J. Zamek-Gliszczynski and L. Zhang, *Nat. Rev. Drug Discov.*, 2010, **9**, 215–36.

49 P. Lefebvre, B. Cariou, F. Lien, F. Kuipers and B. Staels, *Physiol. Rev.*, 2009, **89**, 147–91.

50 R. Pellicciari, G. Costantino, E. Camaioni, B. M. Sadeghpour, A. Entrena, T. M. Willson, S. Fiorucci, C. Clerici and A. Gioiello, *J. Med. Chem.*, 2004, **47**, 4559–69.

51 A. F. Hofmann, L. R. Hagey and M. D. Krasowski, *J. Lipid Res.*, 2010, **51**, 226–46.

52 K. Nakano, K. Aburaya, I. Hisaki, N. Tohnai and M. Miyata, *Chem. Rec.*, 2009, **9**, 124–35.

53 M. Miyata, N. Tohnai, I. Hisaki and T. Sasaki, *Symmetry (Basel).*, 2015, **7**, 1914–1928.

54 Tamura Rui;Miyata Mikiji (eds.), *Advances in Organic Crystal Chemistry - Comprehensive Reviews*, Springer, 2015.

55 S. Ikonen and E. Kolehmainen, *CrystEngComm*, 2010, **12**, 4304.

56 K. Nakano, K. Sada, Y. Kurozumi and M. Miyata, *Chemistry*, 2001, **7**, 209–20.

Electronic Supplementary Information

Table S1: Side chain dihedral angles for three crystallographically independent molecules in compound **2**.

	Molecule 1	**Molecule 2**	**Molecule 3**
C13-C17-C20-C22	-174.0(2)	-172.6(2)	-172.6(2)
C17-C20-C22-C23	-174.0(2)	-171.3(3)	-168.2(2)
C20-C22-C23-C24	72.3(3)	71.3(3)	69.8(3)

C22-C23-C24-N24	-125.9(3)	-115.9(3)	-114.9(3)

Table S2: Crystal data and X-ray experimental details for compounds **1**, **2**, and **3**.

Compound	**1**	**2**	**3**
CCDC No.	1438665	1438666	1438667
Empirical formula	$C_{26}H_{45}NO_2$	$C_{86}H_{147}N_7O_9$	$C_{54}H_{93}N_3O_8$
Formula weight	403.63	1423.10	912.31
Temperature (K)	123.0	120.0	123.0
Crystal system	Monoclinic	Triclinic	Monoclinic
Space group	$P2_1$	P-1	$C2$
Unit cell dimensions: a (Å)	10.7537(3)	7.04914(7)	48.7516(4)
Unit cell dimensions: b (Å)	7.58178(16)	18.4817(2)	7.84759(7)
Unit cell dimensions: c (Å)	14.4627(4)	18.8671(3)	13.90755(11)
Unit cell dimensions: α (°)	90	117.4531(13)	90
Unit cell dimensions: β (°)	97.282(3)	99.2141(11)	90.3673(7)
Unit cell dimensions: γ (°)	90	95.3368(9)	90
Volume / $Å^3$	1169.66(5)	2113.65(5)	5320.68(7)
Z	2	1	4
Density (calculated) mg/m^3	1.146	1.118	1.139
Absorption Coefficient mm^{-1}	0.538	0.557	0.591
F(000)	448	784	2008
Crystal size (mm^3)	0.39 x 0.05 x 0.40	0.28 x 0.07 x 0.05	0.25 x 0.14 x 0.09
θ range for data collection (°)	3.08 to 66.75	4.70 to 66.75	3.18 to 66.75
Reflections collected [R(int)]	11284 [0.0404]	137266 [0.0622]	49802 [0.0384]
Observed reflections [I>2σ(I)]	3790	13789	9012
Data completeness (%)	99.91	99.96	99.98
Data/ restraints/ parameters	4078/1/274	14638/3/941	9284/2/612
Goodness-of-fit on F^2	1.050	1.042	1.058
Final R_1 indices [I>2σ(I)]	R_1 = 0.0421 wR_2 = 0.1084	R_1 = 0.0412 wR_2 = 0.1032	R_1 = 0.0556 wR_2 = 0.1473
Final R indices [all data]	R_1 = 0.0460 wR_2 = 0.1108	R_1 = 0.0444 wR_2 = 0.1063	R_1 = 0.0570 wR_2 = 0.1495
Largest diff. peak/hole ($e.Å^{-3}$)	0.218/ -0.231	0.206/ -0.213	0.810/ -0.505

Equation E1: Evaluation of the viability

$$\text{Viability (\%)} = 100 \cdot \left(\frac{(A_S - A_B)}{(A_C - A_B)} \right)$$

A_S ... absorbance of sample

A_B ... absorbance of background (well without cell)

A_C ... absorbance of control (the cells treated with a serum-free medium without samples)

Figure S1: Effects of 3α-hydroxy-5β-cholan-24-ethylamide (**1**) on cell viability determined by the NR assay after 24 h treatment. The values represent the mean ± SD of three sets of independent experiments.

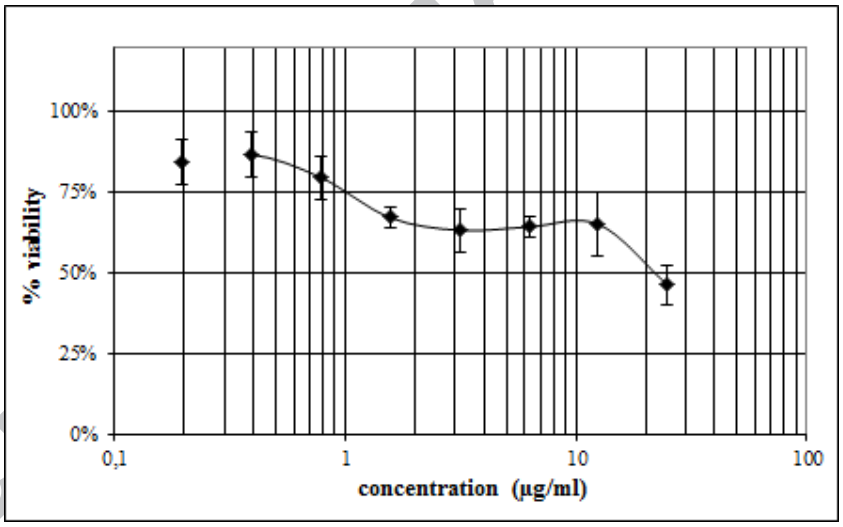

Figure S2: Effects of 3α,12α-dihydroxy-5β-cholan-24-ethylamide (**2**) on cell viability determined by the NR assay after 24 h treatment. The values represent the mean ± SD of three sets of independent experiments.

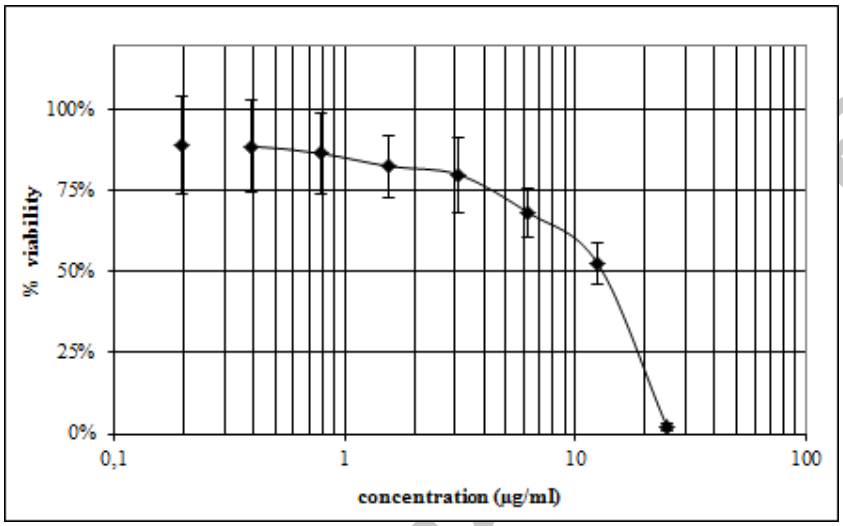

Figure S3: Effects of 3α,7α,12α-trihydroxy-5β-cholan-24-ethylamide (**3**) on cell viability determined by the NR assay after 24 h treatment. The values represent the mean ± SD of three sets of independent experiments.

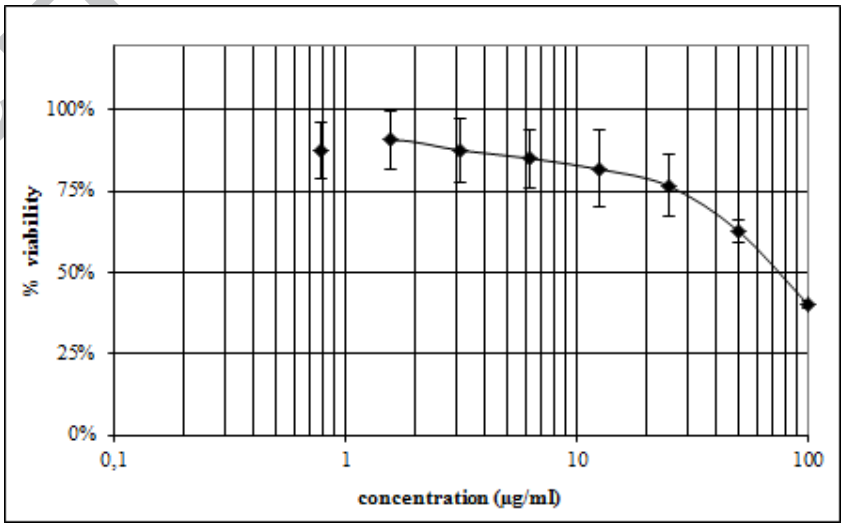

Figure S4: Effects of 3,7,12-trioxo-5β-cholan-24-ethylamide (**4**) on cell viability determined by the NR assay after 24 h treatment. The values represent the mean ± SD of three sets of independent experiments.

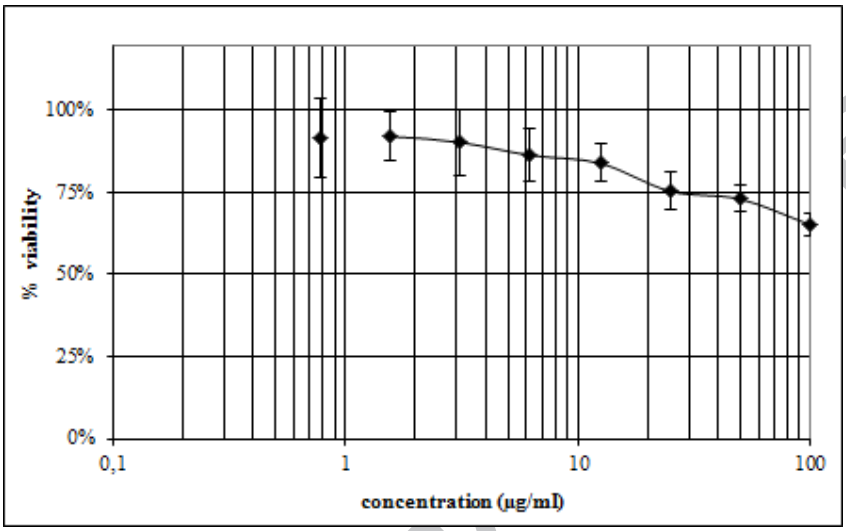

Biocompatible Hydrogelators Based on Bile Acid Ethyl Amides

Riikka Kuosmanen, Rakesh Puttreddy, Roosa-Maria Willman, Ilkka Äijäläinen, Adéla Galandáková, Jitka Ulrichová, Hannu Salo, Kari Rissanen, and Elina Sievänen*

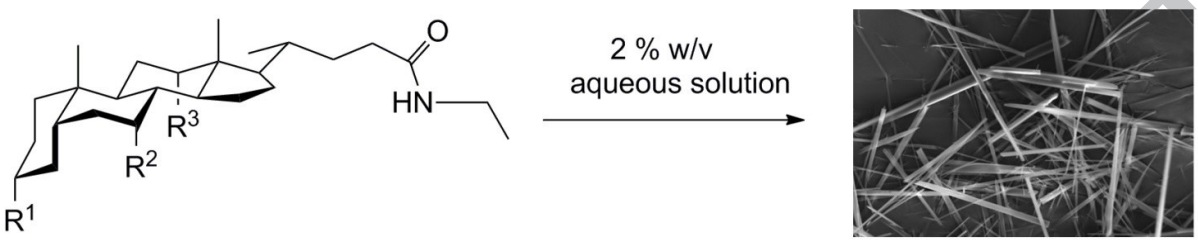

Biocompatible Hydrogelators Based on Bile Acid Ethyl Amides

Riikka Kuosmanen[1], Rakesh Puttreddy[1], Roosa-Maria Willman[1], Ilkka Äijäläinen[1], Adéla Galandáková[2], Jitka Ulrichová[2], Hannu Salo[1], Kari Rissanen[1], and Elina Sievänen[1*]

[1]*University of Jyvaskyla, Department of Chemistry, P.O.Box 35, FI-40014 University of Jyvaskyla, Finland*

[2]*Palacký University in Olomouc, Department of Medical Chemistry and Biochemistry, Hněvotínská 3, CZ-775 15 Olomouc, Czech Republic*

Highlights

- Four new bile acid ethyl amide derivatives were synthesized and characterized in detail.
- Several gel systems, including for the first time bile acid amide derived hydrogels, were formed.
- The properties of the gels were investigated, and the toxicity of the compounds determined.
- The XRD-derived packing patterns may reveal the gel state assembly of the molecules.
- The biocompatibility of these and other bile acid-based hydrogels may be used in biomedicine.